Polyhedron 66 (2013) 153–156

Contents lists available at SciVerse ScienceDirect

Polyhedron

journal homepage: www.elsevier.com/locate/poly

Photoinduced perturbations of the magnetic superexchange in core@shell Prussian blue analogues

Elisabeth S. Knowles [a], Carissa H. Li [b], Matthieu F. Dumont [a,b,1], Marcus K. Peprah [a], Matthew J. Andrus [b], Daniel R. Talham [b,*], Mark W. Meisel [a,*]

[a] Department of Physics and NHMFL, University of Florida, Gainesville, FL 32611-8440, USA
[b] Department of Chemistry, University of Florida, Gainesville, FL 32611-7200, USA

ARTICLE INFO

Article history:
Received 7 January 2013
Accepted 12 March 2013
Available online 21 March 2013

Keywords:
Prussian blue analogues
Photoinduced magnetism
Heterostructures

ABSTRACT

Cubic heterostructured core@shell particles of Prussian blue analogues, composed of a shell (~80 nm thick) of ferromagnetic $K_{0.3}Ni[Cr(CN)_6]_{0.8}\cdot 1.3H_2O$ (**A**), $T_c \sim 70$ K, surrounding a bulk (~ 350 nm) core of photoactive ferrimagnetic $Rb_{0.4}Co[Fe(CN)_6]_{0.8}\cdot 1.2H_2O$ (**B**), $T_c \sim 20$ K, have been studied. Below nominally 70 K, these CoFe@NiCr samples exhibit a persistent photoinduced decrease in low-field magnetization, and these results resemble data from other **BA** core@shell particles and analogous **ABA** heterostructured films. This net decrease suggests that the photoinduced lattice expansion in the **B** layer generates a strain-induced decrease in the magnetization of the NiCr layer, similar to a pressure-induced decrease observed by others in a similar, pure NiCr material and by us in our CoFe@NiCr cubes. Upon further examination, the data also reveal a significant portion of the NiCr shell whose magnetic superexchange, *J*, is perturbed by the photoinduced strain from the CoFe constituent.

1. Introduction

Molecule-based magnets present an intriguing field of materials due to their combination of magnetism with various other physical phenomena. Specifically, materials exhibiting photomagnetic properties provide a vast potential for technological applications. In recent years, Prussian blue analogues (PBAs) have piqued the interest of the molecular magnetism community due to their range of magnetic properties [1]. Although examples exist that are known to order magnetically at or above room temperature [2–4], the feature that distinguishes a particularly appealing subset of PBAs is the phenomenon of a charge-transfer-induced spin transition (CTIST) [5], which is linked with that of persistent photoinduced magnetism (PPIM) [6]. When these properties are combined with long-range magnetic order, the potential for information storage applications begins to emerge.

A quintessential example of such a material is the CoFe–PBA, A_i-$Co[Fe(CN)_6]_j\cdot nH_2O$, where A is a monovalent alkali cation. CoFe–PBAs are well-known to exhibit a photoinduced CTIST up to a temperature of 150 K [7–9], as well as a similar photoinduced transition within the hysteresis of the thermal CTIST near, and even at, room temperature for certain stoichiometries [5,10]. However, these photoinduced effects are weaker above 20 K, which is the critical temperature, T_c, for the long-range magnetic ordering. The fact that the photoeffect in the CoFe is also structural in nature [11] has been utilized to increase the temperature at which photocontrol is possible, by incorporating this material into heterostructures [12–14] with PBAs having higher ordering temperatures and known to be pressure-sensitive [15]. To guide work pursuing room temperature photocontrolled magnetism, we seek a deeper fundamental understanding of the mechanism leading to these novel effects in the heterostructures, focusing here on quantifying the amount of material in the non-photoactive layers that is affected by this photoinduced strain from the CoFe constituent.

In the present study, core and core@shell particles of PBAs (Fig. 1), composed of shells of $K_{0.3}Ni[Cr(CN)_6]_{0.8}\cdot 1.3H_2O$ (**A**), which orders ferromagnetically with $T_c \sim 70$ K [16], surrounding bulk cores of $Rb_{0.4}Co[Fe(CN)_6]_{0.8}\cdot 1.2H_2O$ (**B**), which is photoactive and ferrimagnetic with $T_c \sim 20$ K, have been investigated. The particles presented here possess an average core size of 350 nm on a side and an average shell thickness of 80 nm. These samples exhibit a persistent photoinduced decrease in low-field susceptibility below $T_c \sim 70$ K of the shell, similar to previous results from other **BA** core@shell particles [13] and analogous **ABA** heterostructured films [12,14]. This net decrease is ascribed to the photoinduced lattice expansion in the **B** (CoFe) layer, which generates a strain-induced decrease in the magnetization of the **A** (NiCr) layers, similar to a pressure-induced decrease observed by others in a similar, pure NiCr material, attributed to spin-canting [15]. Upon

* Corresponding authors. Tel.: +1 3523929147.
E-mail addresses: talham@chem.ufl.edu (D.R. Talham), meisel@phys.ufl.edu (M.W. Meisel).
[1] Present address: Children's National Medical Center, 111 Michigan Avenue NW, Washington, DC 20010, USA

0277-5387/$ - see front matter © 2013 Elsevier Ltd. All rights reserved.
http://dx.doi.org/10.1016/j.poly.2013.03.019

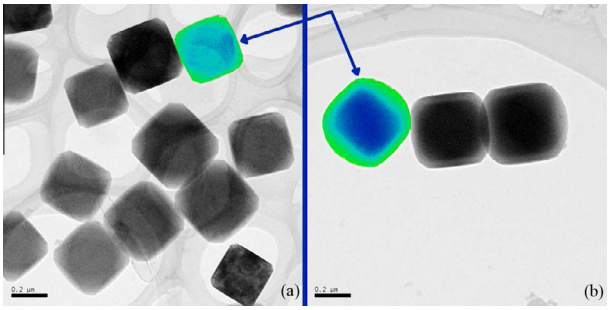

Fig. 1. TEM images of (a) CoFe core and (b) CoFe@NiCr core@shell particles. Scale bars are 200 nm. Selected particles have been color-mapped (black-white to blue-green) to highlight the core@shell contrast.

further examination, the core@shell susceptibility data also reveal a significant portion of the NiCr shell whose magnetic superexchange, *J*, is perturbed with the application of this photoinduced strain from the CoFe core.

2. Experimental

2.1. Synthesis

$K_3Cr(CN)_6$ was synthesized by treating aqueous solutions of potassium cyanide with $CrCl_3{\cdot}6H_2O$ and was used after recrystallization from methanol [17]. Deionized water used in synthetic procedures was obtained from a Barnstead NANOpure system, with a resistivity of at least 17.8 MΩ. All of the other reagents were purchased from Sigma-Aldrich or Fisher-Acros and were used without further purification. The filters used during the synthesis were Fast PES Bottle Top Filters with 0.45 μm pore size (Nalgene).

The synthesis of the core particles was performed at room temperature. An aqueous solution (100 mL) of $CoCl_2{\cdot}6H_2O$ (0.40 mmol, 4.0 mM), and an equal volume of an aqueous solution containing $K_3Fe(CN)_6$ (0.45 mmol, 4.5 mM) were simultaneously added dropwise to 200 mL of nanopure water. To substitute the Rb cation, RbCl (0.80 mmol, 8.0 mM) was included in the $CoCl_2$ solution. The final solution was kept under vigorous stirring for 1 h after all additions were complete. The particles were subsequently filtered under vacuum using a 0.45 μm filter before being washed with ultrapure water and redispersed in 100 mL of water for use in the next step. To isolate the particles, the solution was concentrated by centrifugation and dried under a flow of air.

To prepare the core@shell particles, the core (CoFe) particle suspension was diluted with water to 400 mL. An aqueous solution (50 mL) of $NiCl_2{\cdot}6H_2O$ (0.095 mmol, 1.9 mM) and an aqueous solution (50 mL) of $K_3Cr(CN)_6$ (0.105 mmol, 2.1 mM) were added dropwise (10 mL/h, peristaltic pump) under stirring at room temperature. The final solution was kept under vigorous stirring for 1 h after all additions were complete. Once the addition was complete, the particles were filtered using a 0.45 μm filter and rinsed with ultrapure water. To isolate the particles, the solution was concentrated by centrifugation and dried under a flow of air.

2.2. Instrumentation

Transmission electron microscopy (TEM) was performed on a JEOL-2010F high-resolution transmission electron microscope at 200 kV. TEM grids used were carbon film on a holey carbon support film, 400 mesh, copper from Ted-Pella, Inc. Grids were prepared by dropping 20 μL of a solution containing 5 mg of sample dispersed in 2 mL of EtOH by sonication for 30 min. Energy dispersive X-ray spectroscopy (EDS) was performed with an Oxford Instruments EDS X-ray Microanalysis System coupled to the TEM.

Room temperature powder X-ray diffraction (XRD) was performed on a Bruker DUO diffractometer. Powder samples were packed into 0.3 mm diameter boron-rich thin walled capillary tubes purchased from the Charles Supper Company. Diffraction patterns were collected for $5^\circ \leqslant 2\theta \leqslant 89^\circ$ with a 600 s/image collection time. The raw data generated from the APEX II CCD detector (.raw) were converted to 1D powder patterns (GSAS) using PowDLL converter and analyzed using FullProf Suite software.

Fourier-transform infrared (FTIR) spectroscopy was performed on a Nicolet 6700 Thermo Scientific spectrophotometer. Powder samples were mixed with KBr and pressed into pellets under 20 MPa. Scans (typically 64) were performed between 2200 and 1900 cm^{-1}, in the region of the CN stretching bands, with a precision of 0.482 cm^{-1}. Corresponding scans of a pure KBr pellet were taken as the background measurement.

Magnetization measurements were performed on a Quantum Design MPMS XL-7 superconducting interference device (SQUID) magnetometer using a homemade fiber optic sample rod with a bundle of 10 optical fibers to bring light into the sample space [18]. Powder samples were spread between two pieces of transparent tape and held in transparent drinking straws directly below the optical fibers. Visible white light was supplied by a 150 W tungsten-halogen lamp located at room temperature. The temperature dependence of the low-field susceptibility was measured in an applied field of 100 G while warming the sample from base temperature, 2 K. Isothermal magnetization was measured at 2 K while sweeping the field between 70 and −70 kG. After 8 h of isothermal irradiation at 40 K and 100 G, irradiation was ceased, and the sample was then cooled again to base temperature. All light state measurements were subsequently performed, repeating the same protocol that was used for the dark state measurements.

3. Results and discussion

The TEM images reveal contrast between core and shell in the CoFe@NiCr particles not present for the pure CoFe cores (Fig. 1). In conjunction, EDS line scans of individual particles show Co and Fe content concentrated in the cores, with Ni and Cr content predominately occupying the edges [19]. The FTIR spectra display an additional CN stretching frequency, near 2175 cm^{-1}, arising after the growth of the NiCr shell, consistent with observations for the pure NiCr material. Powder XRD patterns also present two distinct lattice constants consistent with the room temperature, single-phase CoFe [11] and NiCr [16] materials, respectively, while only the CoFe phase is exhibited in the core particles (Fig. 2).

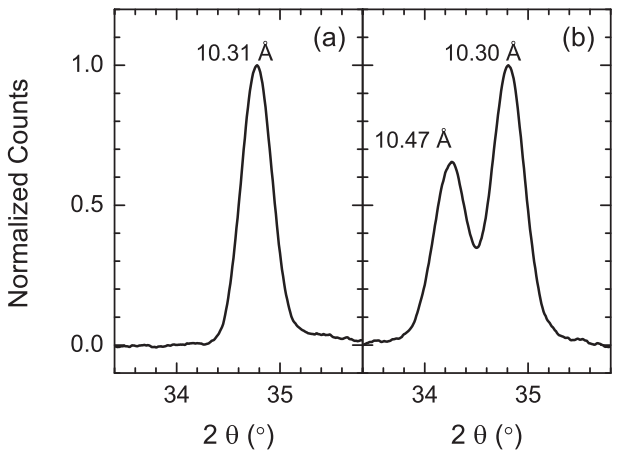

Fig. 2. XRD [400] peaks of the (a) CoFe core and (b) CoFe@NiCr core@shell particles, normalized to the CoFe peak, as a function of 2θ.